

# Evaluation of kinetic parameters of the Dalat nuclear research reactor with LEU fuel

Duc-Tu Dau\*

Dalat Nuclear Research Institute  
Vietnam Atomic Energy Institute  
Dalat, Lamdong 670000, Viet Nam  
tudd.re@dnri.vn

Nhi-Dien Nguyen

Dalat Nuclear Research Institute  
Vietnam Atomic Energy Institute  
Dalat, Lamdong 670000, Viet Nam

Hoai-Nam Tran\*\*

Phenikaa Institute for Advanced Study  
PHENIKAA University,  
Hanoi 12116, Viet Nam  
nam.tranhoai@phenikaa-uni.edu.vn

**Abstract**—Kinetic parameters of the Dalat Nuclear Research Reactor (DNRR) was evaluated using the MCNP6.3 code and new nuclear data libraries (ENDF/B-VIII.0 and JENDL-5.0). Calculations were performed for the core configuration of 92 low-enriched uranium (LEU) fuel bundles for obtaining the effective delayed neutron fraction  $\beta_{eff}$ , the neutron generation time  $\Lambda$  and the prompt neutron lifetime  $l_p$ . Two methods were used to calculate the  $\beta_{eff}$ : the adjoint weighted method and the prompt method. To calculate the  $l_p$ , the adjoint weighted method and the  $1/v$  absorber insertion method were used. The values of  $\beta_{eff}$ ,  $\Lambda$  and ( $l_p$ ) at the beginning of cycle (BOC) obtained with the adjoint weighted method and the ENDF/B-VIII.0 library are 750 pcm, 86.80  $\mu$ s and 78.86  $\mu$ s. Comparing between the methods and the libraries, the discrepancies are within 1%. Some isotopes having major contribution to the sensitivities and uncertainties of the  $\beta_{eff}$  are AL-27, H-1, U-235, Be-9 and O-16.

**Index Terms**—Kinetic parameter, DNRR, MCNP6, ENDF/B-VIII.0, JENDL-5.0

## I. INTRODUCTION

The Dalat Nuclear Research Reactor (DNRR) is a 500 kW pool-type research reactor, operated by Dalat Nuclear Research Institute (Dalat, Vietnam). In 1983, the DNRR core was upgraded from the TRIGA-MARK II research reactor with the power of 250 kW and loaded with highly enriched uranium (HEU) fuel ( $^{235}\text{U}$  enrichment of 35 wt%) of the Russian WWR-M2 fuel type. In 2011, the core was completely converted to low-enriched uranium (LEU) fuel with the  $^{235}\text{U}$  enrichment of 19.75 wt% [1]. The operation of the DNRR is essential for the development of many scientific activities and applications including nuclear physics, nuclear engineering, biology and agriculture, as well as radioactive isotope production for medical and industrial applications [1]–[6].

Kinetic parameters of the reactor core such as effective delayed neutron fraction, neutron generation lifetime and prompt neutron lifetime are among important core characteristics related to reactor safety, control rod and transient analysis. Delayed neutrons in a reactor core are generated during the decay process of radionuclides which are the products of fission reactions. For example, neutrons emitted during the beta decay of iodine, bromine and other nuclei. The temporal delay of neutrons is dependent on the lifetime

of fission products. Though the delayed neutrons occupy less than 1% of the total neutron population, they have a significant effect on the safety-related characteristics of the reactor core. Thus, precise evaluation of the kinetic parameters contribute to improve the safety and the effective operation of the reactor. Several factors would involve in the uncertainty in the evaluation of the kinetic parameters, such as computational codes, implemented methods, core simulation model, isotopic compositions of materials and nuclear data libraries. Pinem et al reported the kinetic parameters of the RSG-GAS research reactor using several methods implemented in the Serpent 2 code and the ENDF/B-VII.1 and ENDF/B-VIII.0 data libraries [7]. A previous work performed the sensitivity and uncertainty analysis for the criticality of the DNRR core with HEU fuel using several versions of ENDF/B and JENDL [2]. Since the core physics and safety-related analysis of the DNRR have been performed mainly with the ENDF/B and JENDL data libraries, it is of high beneficial to conduct the calculations with the latest versions of the library systems, i.e., ENDF/B-VIII.0 (released in 2018) and JENDL-5.0 (released in 2021).

In the present work, calculations of the kinetic parameters of the DNRR core with LEU fuel have been conducted using the MCNP6 code [8] and the latest ENDF/B and JENDL data libraries [9], [10]. Two methods were used to calculate the  $\beta_{eff}$ : the adjoint weighted method and the prompt method. Whereas, to calculate the  $l_p$ , the adjoint weighted method and the  $1/v$  absorber insertion method were used. The kinetic parameters were evaluated at both the beginning of cycle (BOC) which was 46.88 days of operation, and the end of cycle (EOC) which was 933.2 operational days of the DNRR. Comparison between the methods and between the data libraries was performed and presented.

## II. THE DNRR AND CALCULATION MODEL

### A. The DNRR

The DNRR core consists of a cylindrical aluminum tank of 6.26 m in height and 1.98 m in diameter. The active core has a cylindrical shape with the height of 60 cm and the diameter of 44.2 cm. The core includes 121 hexagonal cells for loading fuel bundles, control rods, irradiation channels and beryllium blocks. The control rod system includes: one automatic regulating rod (AR), four shim rods (ShR) and two

This research is funded by Vietnam National Foundation for Science and Technology Development (NAFOSTED) under grant 103.04-2023.116.

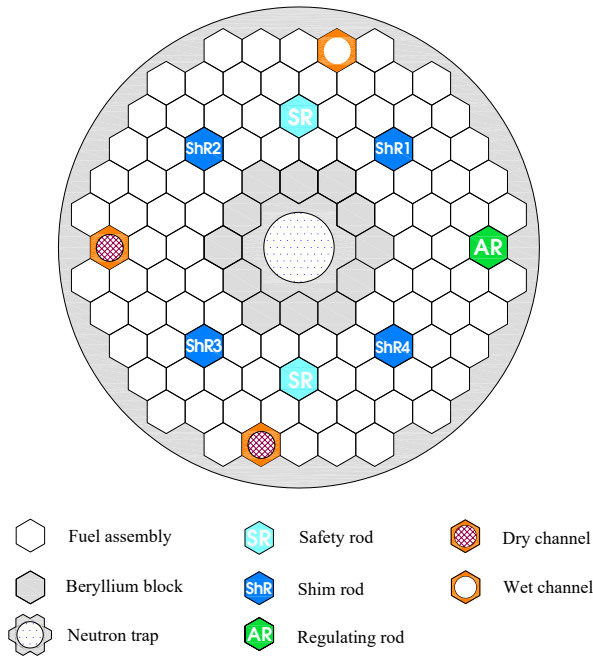


Fig. 1. Configuration of the DNRR core with 92 LEU fuel bundles.

safety rods (SR). The absorption length of the control rods is 65 cm to completely cover the active core. Dry channel and wet channel are covered by aluminum cylinders with the thickness of 0.5 mm. The neutron trap at the core center is a water cylinder with 6.5 cm in diameter and 60 cm in length surrounded by six beryllium blocks. The beryllium block has the same outer shape as the fuel bundle. A beryllium ring is located between the active core and the graphite reflector and serves as an additional reflector. The thickness of the graphite reflector is 30.5 cm. Further description of the DNRR core can be found in [1]–[6]. Fig. 1 shows the core configuration of the DNRR consisting of 92 LEU fuel bundles [1]. Table I provides the main design specifications of the DNRR core and the VVR-M2 LEU fuel [1].

Fig. 2 displays the cross-sectional view and the design parameters of the LEU fuel bundle. The LEU fuel bundle has three concentric annular tubes, along with a header and a tail. The outermost fuel tube is hexagonal, with parallel sides of 32 mm in width. Two inner fuel elements have circular shapes, with the outer diameters of 22 mm and 11 mm, respectively. The fuel employed comprises a mixture of uranium dioxide ( $\text{UO}_2$ ) and aluminum (Al).

### B. Calculation model

Kinetic parameters of the DNRR core with LEU fuel were calculated using the MCNP6.3 code [8] and the ENDF/B-VIII.0 and JENDL-5.0 nuclear data libraries [9], [10]. Fig. 3 displays the vertical and horizontal cross-sectional views of the DNRR core model in the MCNP6.3 code. The model is expanded from the active core to the reactor tank, with the dimensions of 198 cm in diameter and 184.5 cm in height. The

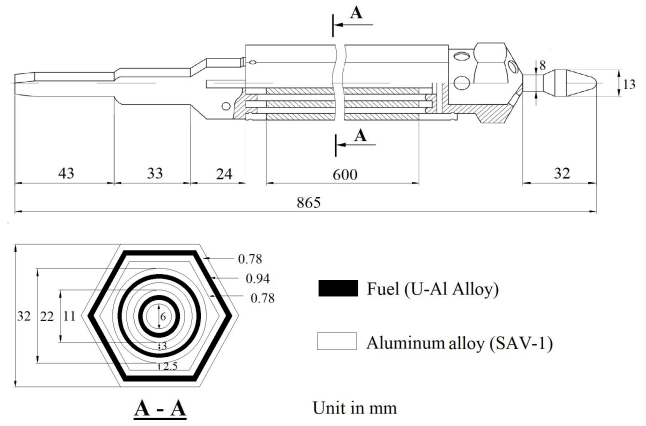


Fig. 2. Cross-sectional view of the Russian VVR-M2 type LEU fuel bundle.

TABLE I  
DESIGN SPECIFICATIONS OF THE DNRR CORE WITH LEU FUEL.

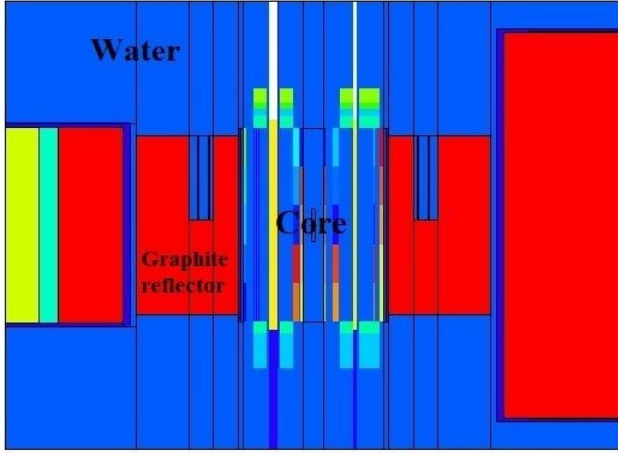
Parameter	Value
Reactor	
Reactor type	Pool type
Fuel type	Russian VVR-M2
Cooling system	Natural convection
Moderator and coolant	Water
Reflector	Graphite, beryllium and water
Nominal power (kW)	500
Core	
Number of assemblies	92
Regulating rod (Stainless steel)	1
Shim rod ( $\text{B}_4\text{C}$ )	4
Safety rod ( $\text{B}_4\text{C}$ )	2
Beryllium rod	12
Irradiation channel	4
Average burnup at EOC (Percent loss of $^{235}\text{U}$ )	22
Fuel	
$^{235}\text{U}$ enrichment (wt%)	19.75
Number of fuel elements in a bundle	3
Outermost element (Hexagonal shape)	1
Inner elements (Circular shape)	2
Fuel element thickness (mm)	2.5
Fuel meat thickness (mm)	0.94
Cladding thickness (mm)	0.78
Fuel clad material	Al
Fuel meat material	Al-U alloy
Coolant channel width (mm)	2.5–3
Total length of a fuel bundle (mm)	865
Active fuel length (mm)	600

MCNP6 calculations were conducted with 200 cycles and  $10^5$  neutron histories per cycle for obtaining the statistical error of  $k_{eff}$  less than 20 pcm. The kinetic parameters were calculated at the beginning of cycle (BOC) and the end of cycle (EOC) to evaluate the effect of fuel burnup.

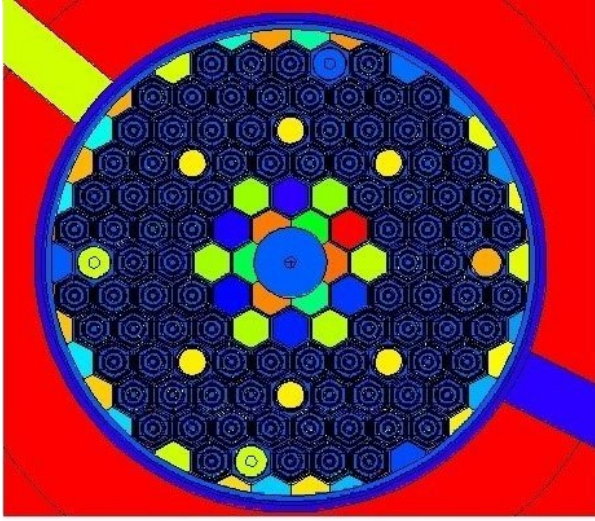
## III. KINETIC PARAMETERS

### A. Effective delayed neutron fraction ( $\beta_{eff}$ )

Radionuclides emitting delayed neutrons are called the delayed neutron precursors. Depending on the half-life of the radionuclides, the delayed neutron intensity and their effect



a) Vertical cross-section



b) Horizontal cross-section

Fig. 3. Vertical (a) and horizontal (b) cross-sectional views of the DNRR core model in the MCNP6 code.

also change with time. Thus, the delayed neutron precursors are divided into six groups based on their half-life. The delayed neutron fraction in a precursor,  $\beta_i$ , is defined as the ratio of the delayed neutron in this group to the total neutron generated in a fission reaction. Then, the effective delayed neutron fraction, denoted as  $\beta_{eff}$ , is the sum of the delayed neutron fractions over the six precursors. Two methods were employed to calculate the effective delayed neutron fraction  $\beta_{eff}$ : the adjoint weighted method and the prompt method. The equation to calculate the effective delayed neutron fraction  $\beta_{eff}$  is written as [11]:

$$\beta_{eff} = \frac{\langle \phi^+, \mathbf{B}\phi \rangle}{\langle \phi^+, \mathbf{F}\phi \rangle}, \quad (1)$$

where,

$\phi$  and  $\phi^+$  are the forward and adjoint neutron fluxes, respectively;

$\mathbf{B}$  is the delayed neutron operator;

$\mathbf{F}$  is the fission term operator;

$\langle \cdot \rangle$  is the integration over space and energy.

B. Neutron generation time ( $\Lambda$ ) and prompt neutron lifetime ( $l_p$ )

The neutron generation time  $\Lambda$ , and the prompt neutron lifetime  $l_p$  are calculated based on the following equations [11]:

$$\Lambda = \frac{\langle \phi^+, \frac{1}{v}\phi \rangle}{\langle \phi^+, \mathbf{F}\phi \rangle}, \quad (2)$$

and

$$l_p = \frac{\langle \phi^+, \frac{1}{v}\phi \rangle k_{eff}}{\langle \phi^+, \mathbf{F}\phi \rangle}, \quad (3)$$

where,  $k_{eff}$  is the effective multiplication factor;  $v$  is the neutron speed.

The prompt neutron lifetime  $l_p$  was calculated using the adjoint weighted method and the  $1/v$  absorber insertion method [12]. The adjoint weighted method has been implemented in the KOPTS card of the MCNP code. The  $1/v$  absorber insertion method involved the introduction of a small addition of  $^{10}\text{B}$  as a perturbation in the core materials. The appearance of the absorber content results in a negative change of the reactivity. The negative reactivity insertion is calculated as:

$$\rho = \frac{\Delta k}{k} = \frac{1}{k_{eff,u}} - \frac{1}{k_{eff,p}}, \quad (4)$$

where:

$k_{eff,u}$  is the effective multiplication factor without the B-10 addition (unperturbed);

$k_{eff,p}$  is the effective multiplication factor with additional B-10 content (perturbed).

The  $k_{eff,p}$  is calculated by changing the  $^{10}\text{B}$  content added to the core materials. The reactivity insertion due to the addition of the  $^{10}\text{B}$  content is:

$$-\frac{\Delta k}{k} = N \cdot \sigma_0 \cdot v_0 \cdot l'_p \quad (5)$$

where,

$N$  is the atomic density of the  $^{10}\text{B}$  absorber ( $\#atoms/(b.cm)$ );

$\sigma_0$  is the thermal neutron absorption cross section of the absorber;

$v_0$  is the speed of thermal neutrons;

$l'_p$  is the prompt neutron lifetime when  $^{10}\text{B}$  absorber is added.

The prompt neutron lifetime  $l_p$  is calculated when the  $^{10}\text{B}$  content approaches zero:

$$l_p = \lim_{N \rightarrow 0} l'_p = \lim_{N \rightarrow 0} \left( -\frac{\Delta k}{k} \frac{1}{N \cdot \sigma_0 \cdot v_0} \right) \quad (6)$$

In the present work, the  $^{10}\text{B}$  content was added uniformly to all core materials with the concentration from  $4.0 \times 10^{-9}$  to  $15.0 \times 10^{-9} atoms/(b.cm)$ . The  $k_{eff,p}$  value was then calculated at each step of the  $^{10}\text{B}$  contents for determining the linear dependence of the reactivity with the  $^{10}\text{B}$  content. The  $l_p$  is obtained when the  $^{10}\text{B}$  content approaches to zero.

### C. Sensitivity of the effective delayed neutron fraction

Sensitivity and uncertainty analysis has been performed to investigate the contribution of major nuclides and nuclear reactions to the uncertainty sources of the kinetic parameters. The sensitivity of the  $\beta_{eff}$  is calculated as follows [13]:

$$S_{\sigma}^{\beta_{eff}} = \frac{\sigma}{\beta_{eff}} \frac{\partial \beta_{eff}}{\partial \sigma} = \frac{(1 - \beta_{eff})}{\beta_{eff}} (S_{\sigma}^k - S_{\sigma}^{k_p}), \quad (7)$$

where,  $S_{\sigma}^k$  and  $S_{\sigma}^{k_p}$  are the sensitivities of  $k$  and  $k_p$ , respectively, obtained from the linear perturbation theory. The uncertainty of the  $\beta_{eff}$  to the nuclear data was computed using the sensitivity profile and the data covariance matrix following the uncertainty propagation rule. The formula to calculate the uncertainty of  $\beta_{eff}$  is given as [14]:

$$U_{\sigma}^{\beta_{eff}} = \sqrt{[S_{\sigma}^{\beta_{eff}}]^T [C] [S_{\sigma}^{\beta_{eff}}]}, \quad (8)$$

where,  $[C]$  is the data covariance matrix of the nuclear reactions for each isotope obtained by using the NJOY2021 code with 44 energy groups.

## IV. RESULTS AND DISCUSSION

### A. Effective delayed neutron fraction

The MCNP6.3 calculations were setup to estimate the  $k_{eff}$  of the DNRR core with 92 LEU fuel bundles with the standard deviation ( $1\sigma$ ) of 15–21 pcm. Table II shows the  $\beta_{eff}$  values of the DNRR core at BOC and EOC in comparison between the adjoint weighted method and the prompt method, as well as between the two data libraries. Fig. 4 depicts the dependence of the  $\beta_{eff}$  on burnup. As shown in Fig. 4, the  $\beta_{eff}$  decreases more rapidly in the first 200 effective full power days (EFPDs), which is then followed by a gradual decline. The  $\beta_{eff}$  decreases from BOC to EOC (800 EFPDs) by about 46–52 pcm. The adjoint weighted method predicts the  $\beta_{eff}$  values of 750 and 760 pcm at BOC corresponding to the use of ENDF/B-VIII.0 and JENDL-5.0, respectively. The values at EOC are 704 and 708 pcm, respectively. One can notice that the  $\beta_{eff}$  values calculated using the adjoint weighted method with JENDL-5.0 are greater than that with ENDF/B-VIII.0 at both BOC and EOC by 4–10 pcm. The prompt method estimated the  $\beta_{eff}$  lower than the adjoint weighted method by about 8–12 pcm. Comparing between the two methods, a good agreement was found with the discrepancy less than 1.6%. The discrepancy between the two data libraries is less than 1.7%.

### B. Neutron generation time and prompt neutron lifetime

The values of neutron generation time,  $\Lambda$ , at BOC and EOC obtained by using the adjoint weighted method and the ENDF/B-VIII.0 library are 86.80 and 82.58  $\mu s$ , respectively. These values obtained with the JENDL-5.0 library are 86.99 and 82.41  $\mu s$ , respectively. The results implies that a good agreement between the two libraries in predicting the  $\Lambda$  values.

Fig. 5 presents the prompt neutron lifetime  $l_p$  as a function of burnup obtained by the adjoint weighted method. The  $l_p$  increases linearly with burnup due to the decrease of the

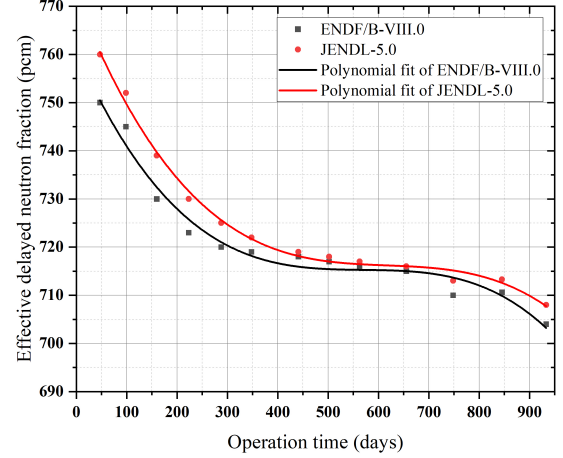


Fig. 4. Effective delayed neutron fraction  $\beta_{eff}$  versus the burnup time using the adjoint weighted method.

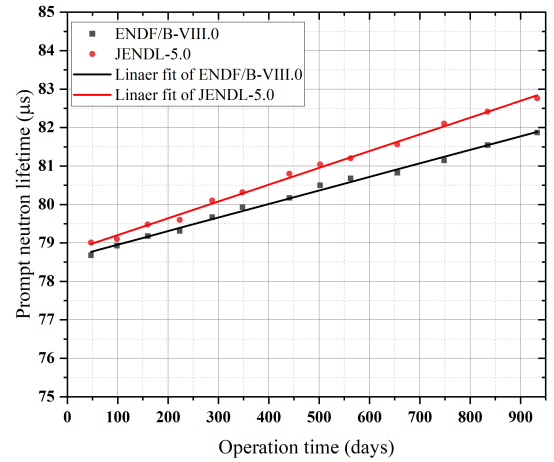


Fig. 5. Prompt neutron lifetime  $l_p$  versus burnup time using the adjoint weighted method.

production rate. The  $l_p$  values at BOC and EOC are 78.68 and 81.87  $\mu s$ , respectively, with the use of ENDF/B-VIII.0. The values obtained with JENDL-5.0 are greater by about 1%. Figs. 6 and 7 depict the determination of the  $l_p$  values using the  $1/v$  absorber insertion method at BOC and EOC, respectively, by varying the  $^{10}B$  concentration from  $4.0 \times 10^{-9}$  to  $15.0 \times 10^{-9}$  atoms/(b.cm). As shown in Table III the  $l_p$  at BOC obtained with ENDF/B-VIII.0 and JENDL-5.0 are 78.54 and 79.72  $\mu s$ , respectively. Whereas, the  $l_p$  values at EOC are 81.66 and 82.98  $\mu s$ , respectively. Comparing between the two methods and between the two data libraries, the discrepancy of the  $l_p$  values is within 1%.

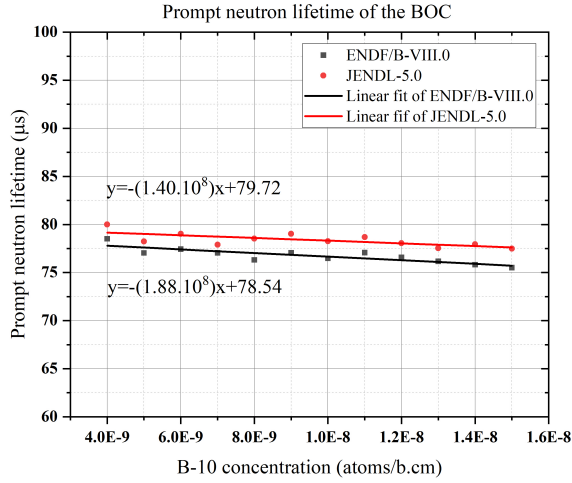


Fig. 6. Prompt neutron lifetime as a function of B-10 concentration at BOC.

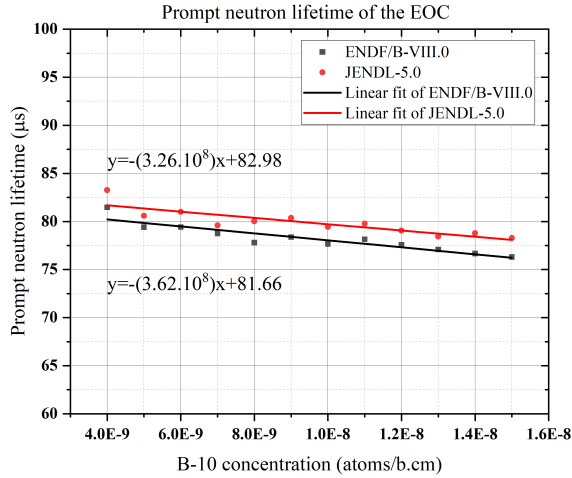


Fig. 7. Prompt neutron lifetime as a function of B-10 concentration at EOC.

TABLE II  
EFFECTIVE DELAYED NEUTRON FRACTION  $\beta_{eff}$  (PCM).

Method	ENDF/B-VIII.0		JENDL-5.0	
	BOC	EOC	BOC	EOC
Adjoint weighted	750±6	704±22	760±4	708±21
Prompt method	742±6	712±27	748±9	700±18

TABLE III  
THE PROMPT NEUTRON LIFETIME  $l_p$  ( $\mu s$ ).

Method	ENDF/B-VIII.0		JENDL-5.0	
	BOC	EOC	BOC	EOC
Adjoint weighted	78.68±0.14	81.87±0.15	79.01±0.11	82.76±0.15
1/v insertion	78.54±0.17	81.66±0.18	79.72±0.45	82.98±0.19

### C. Sensitivity analysis

Sensitivity and uncertainty analysis were performed for the  $\beta_{eff}$  with the two data libraries. Table V shows the sensitivities of the  $\beta_{eff}$  to the isotopes and reactions with major contribution, i.e., the absolute values greater than 0.1%. Table VI provide the major contributions to the uncertainties of the  $\beta_{eff}$ . It is noticed that several isotopes with the most contributions to the sensitivities and uncertainties of the  $\beta_{eff}$  of the DNRR core are AL-27, H-1, U-235, and C-12.

TABLE IV  
COMPARISON OF THE KINETIC PARAMETERS CALCULATED BY THE ADJOINT WEIGHTED METHOD.

Parameter	ENDF/B-VIII.0		JENDL-5.0	
	BOC	EOC	BOC	EOC
$\beta_{eff}$ (pcm)	750 ± 6	704 ± 22	760 ± 4	708 ± 21
$\Lambda$ ( $\mu s$ )	86.80 ± 0.14	82.58 ± 0.45	86.99 ± 0.11	82.41 ± 0.45
$l_p$ ( $\mu s$ )	78.68 ± 0.14	81.87 ± 0.15	79.01 ± 0.11	82.76 ± 0.15

TABLE V  
THE  $\beta_{eff}$  SENSITIVITIES FOR THE REACTIONS OF THE MAIN ISOTOPES.

Reaction	ENDF-VIII.0		JENDL-5.0	
	BOC	EOC	BOC	EOC
AL-27 Elastic	1.385E+0	1.182E-1	6.346E-1	1.580E+0
H-1 Elastic	7.230E-1	-1.056E+0	-6.913E-1	1.610E+0
U-235 Fission	6.394E-1	-5.859E-2	-2.287E-1	-3.958E-1
C-12 Elastic	1.538E-1	1.460E+0	-3.533E-1	2.496E-1
U-235 n,gamma	1.160E-1	-2.850E-2	-2.286E-2	-7.066E-2
H-1 n,gamma	7.425E-2	-1.166E-1	-1.096E-1	-8.480E-2
U-235 Total nu	-1.514E-3	5.085E-2	3.014E-3	4.947E-2
AL-27 n,gamma	-7.292E-3	-2.022E-2	-1.781E-2	-2.828E-2
U-238 n,gamma	-1.683E-2	-4.622E-2	-7.870E-2	8.640E-3
AL-27 Inelastic	-5.670E-2	-1.259E-1	-1.658E-1	-1.294E-1
Be-9 Elastic	-1.454E-1	-1.015E-1	9.499E-2	1.316E-1
O-16 Elastic	-5.012E-1	-1.380E-1	-1.057E+0	1.992E+0
Be-9 n,2n	-8.341E-1	-1.015E-1	9.499E-2	1.316E-1

TABLE VI  
THE  $\beta_{eff}$  UNCERTAINTIES IN THE DECREASING DIRECTION OF BOC OF ENDF/B-VIII.0 (%).

Reaction	ENDF/B-VIII.0		JENDL-5.0	
	BOC	EOC	BOC	EOC
AL-27 (n,elastic)	4.93	3.16	-	-
Be-9 (n,2n)	3.43	0.22	-	-
Al-27 (n,inelastic)	1.54	2.83	-	-
O-16 (n,elastic)	0.77	0.55	0.44	0.69
U-235 (n,f)	0.34	0.11	0.29	0.23
Be-9 (n,elastic)	0.21	0.22	-	-
H-1 (n,elastic)	0.19	0.45	0.25	1.19
U-235 (total $\nu$ )	0.17	0.07	0.17	0.11
H-1 (n, $\gamma$ )	0.15	0.24	0.23	0.18
U-238 (n, $\gamma$ )	0.12	0.08	0.10	0.06
C-12 (n,elastic)	0.11	0.88	-	-

### V. CONCLUSIONS

Kinetic parameters of the DNRR core consisting of 92 LEU fuel bundles were evaluated using the MCNP6.3 code and the ENDF/B-VIII.0 and JENDL-5.0 data libraries, including the

effective delayed neutron fraction  $\beta_{eff}$ , the neutron generation  $\Lambda$  and the prompt neutron lifespan ( $l_p$ ). The values of  $\beta_{eff}$ ,  $\Lambda$  and ( $l_p$ ) at BOC obtained with the adjoint weighted method and ENDF/B-VIII.0 are 750 pcm, 86.80  $\mu s$  and 78.86  $\mu s$ . The discrepancies of these values obtained with other methods and library are within 1%. The isotopes with major contribution to the sensitivities and uncertainties of the  $\beta_{eff}$  are AL-27, H-1, U-235, Be-9 and O-16.

## REFERENCES

- [1] N. D. Nguyen (Ed.), "Safety Analysis Report for the Dalat Nuclear Research Reactor," Technical Report, Nuclear Research Institute, Vietnam Atomic Energy Commission, 2003.
- [2] T. N. Chu, G.T.T. Phan, L. Q. L. Tran, T. H. Bui, Q. B. Do, D. T. Dau, et al., "Sensitivity and uncertainty analysis of the first core of the DNRR using MCNP6 and new nuclear data libraries," Nucl. Eng. Des., vol. 419, 112986, 2024.
- [3] Q. B. Do, G. T. T. Phan, K. C. Nguyen, Q. H. Ngo, H. N. Tran, "Criticality and rod worth analysis of the DNRR research reactor using the SRAC and MCNP5 codes," Nucl. Eng. Des., vol. 343, 2019, pp. 197–209. <http://dx.doi.org/10.1016/j.nucengdes.2019.01.011>.
- [4] Q. B. Do, H. N. Tran, Q. H. Ngo, G. T. T. Phan, "Determination of fuel burnup distribution of a research reactor based on measurements at subcritical conditions," Nucl. Sci. Tech., vol. 29, p. 174, 2018. <http://dx.doi.org/10.1007/s41365-018-0511-0>.
- [5] G. T. T. Phan, Q. B. Do, Q. H. Ngo, T. A. Tran, H. N. Tran, "Application of differential evolution algorithm for fuel loading optimization of the DNRR research reactor. Nucl. Eng. Des., vol. 362, 110582, 2020. <http://dx.doi.org/10.1016/j.nucengdes.2020.110582>.
- [6] G. Phan, H. N. Tran, K. C. Nguyen, V. P. Tran, V. K. Hoang, P. N. V. Ha, H. A. T. Kiet, "Comparative analysis of the Dalat nuclear research reactor with HEU fuel using SRAC and MCNP5," Sci. Technol. Nucl. Install. 2017, 2615409. <http://dx.doi.org/10.1155/2017/2615409>, 10.
- [7] S. Pinem, L. P. Hong, W. Luthfi, T. Surbakti, D. Hartanto, "Evaluation of kinetic parameters RSG-GAS reactor equilibrium Silicide Core using continuous-energy Monte Carlo Serpent 2 Code," Nucl. Sci. Eng., 1–15, 2024. <https://doi.org/10.1080/00295639.2023.2284433>
- [8] J. A. Kulesza, T. R. Adams, J. C. Armstrong, S. R. Bolding, F. B. Brown, J. S. Bull, et al., "MCNP@ Code Version 6.3.0 Theory & User Manual," Los Alamos National Laboratory Tech. Rep. LA-UR-22-30006, Rev. 1. Los Alamos, NM, USA. September 2022.
- [9] Brown, D., Chadwick, M., Capote, R., Kahler, A., Trkov, A., Herman, et al., "ENDF/B-VIII.0: The 8th major release of the nuclear reaction data library with cielo-project cross sections, new standards and thermal scattering data. Nucl. Data Sheets, vol. 148, pp. 1–142, 2018. <http://dx.doi.org/10.1016/j.nds.2018.02.001>.
- [10] O. Iwamoto, N. Iwamoto, S. Kunieda, F. Minato, S. Nakayama, Y. Abe, et al., "Japanese evaluated nuclear data library version 5: JENDL-5," J. Nucl. Sci. Technol. vol. 60, pp. 1–60, 2023. <http://dx.doi.org/10.1080/00223131.2022.2141903>.
- [11] Brian Kiedrowski, Forrest Brown, Paul Wilson, "Calculating kinetics parameters and reactivity changes with continuous-energy monte carlo," American Nuclear Society PHYSOR, 2010.
- [12] A.L. Hanson, D.J. Diamond "Prompt Neutron Lifetime for the NBSR Reactor," Transactions of the American Nuclear Society, Vol. 106, 2012.
- [13] I.-A. Kodeli, "Sensitivity and uncertainty in the effective delayed neutron fraction ( $\beta_{eff}$ )," Nucl. Instr. Methods Phys. Res. A, vol. 715, pp. 70–78, 2013.
- [14] R. E. MacFarlane, D. W. Muir, R. M. Boicourt, A. C. Kahler, J. L. Conlin, W. Haeck "The NJOY Nuclear Data Processing System," Los Alamos National Laboratory, 2019.